PROCEEDINGS OF SCIENCE

Measurement of low-mass dielectrons in pp, p–Pb and Pb–Pb collisions with the ALICE experiment at the LHC

Alberto Caliva* **for the ALICE Collaboration**
NIKHEF, Universiteit Utrecht
E-mail: alberto.caliva@cern.ch

Abstract

Dielectrons are a unique tool to probe several stages of the space-time evolution of the hot and dense system created in ultra-relativistic heavy ion collisions. They carry unaffected information since once produced they escape the medium with negligible final state interaction. The low-mass region of the dielectron spectrum (below the ρ-meson mass) is interesting for the study of virtual direct photons and possible in-medium modifications of low-mass vector meson spectral functions, that are connected to the partial chiral symmetry restoration expected at high temperature. ALICE is a detector at the LHC dedicated to the study of heavy-ion collisions. Its excellent tracking and particle identification capabilities make this experiment well suited for dielectron measurements. Electrons are reconstructed in the ALICE central barrel using the Inner Tracking System (ITS) and the Time Projection Chamber (TPC). These detectors are also used for the particle identification together with the Time-Of-Flight detector (TOF).

We present the ALICE dielectron measurements in pp collisions at 7 TeV (cocktail comparison and virtual photon extraction), in p–Pb collisions at 5.02 TeV (cocktail comparison) and the current status in central (0–10%) and semi-central (20–50%) Pb–Pb collisions at 2.76 TeV. We also discuss the perspectives for the next runs (Run 2 and Run 3) and the scenario after the ITS and TPC upgrades.

7th International Conference on Physics and Astrophysics of Quark Gluon Plasma
1-5 February , 2015
Kolkata, India

*Speaker.

PoS(ICPAQGP2015)069

1. Introduction

Electromagnetic radiation is emitted abundantly and continuously during all the stages of ultra-relativistic heavy ion collisions [1]. A deconfined phase of quarks and gluons is created in these collisions, called quark–gluon plasma (QGP) [2]. Photons interact only through the electromagnetic force such that they pass through the medium almost unscathed, thus carrying direct information on the production sources. Photons originating from different stages are experimentally indistinguishable, so theoretical models are employed to separate the different components of the total photon spectrum. High–p_{T} region of the spectrum is dominated by prompt photons, produced in the initial hard scattering between colliding partons. This component is well described in terms of perturbative Quantum Chromodynamics (pQCD) [3]. The low-intermediate region of the p_{T} spectrum is mainly populated by thermal photons [4], which give information on the effective average temperature of the system. This component includes contributions from all of the collision stages, with large variations in photon emmitance and medium temperature, and is blue shifted due to the rapidly expanding fireball. Dielectrons produced by internal conversion of virtual direct photons provide several advantages in the measurement of electromagnetic radiation compared to real photons. The dielectron invariant mass spectrum is Lorentz invariant and hence it is not affected by the Doppler shift. Different regions of the dielectron spectrum are particularly sensitive to different stages of the collision, so that the dielectron spectrum can be used as a chronometer of the collision. The low mass region ($m_{\mathrm{ee}} < m_{\rho}$) is particularly interesting since it allows to extract the fraction of virtual photons in the zero mass limit, thus representing a complementary and independent measurement of the real photon spectrum. Moreover it allows the measurement of possible in-medium modification of low-mass vector mesons, directly connected to a partial chiral symmetry restoration in the QGP phase [5]. Low–mass dielectrons are also sensitive to the $\mathrm{c\bar{c}}$ cross section and at higher masses (between the ϕ and the J/ψ mesons) dielectrons are also sensitive to the $\mathrm{b\bar{b}}$ cross-section [6].

In these proceedings, the preliminary results on the dielectron invariant mass, transverse momentum spectrum and the virtual photon extraction in pp collisions at $\sqrt{\mathrm{s}} = 7$ TeV are presented. The invariant mass spectrum and pair transverse momentum ($p_{\mathrm{T}}^{\mathrm{ee}}$) spectra in p–Pb collisions at $\sqrt{\mathrm{s_{NN}}} = 5.02$ TeV are compared to the expected contributions from hadronic sources. The current status of the analysis on the dielectron yields and elliptic flow v_2 in Pb–Pb collisions at $\sqrt{\mathrm{s_{NN}}} = 2.76$ TeV are presented together with the perspectives for Run 3 after the Inner Tracking System (ITS) [7] and Time Projection Chamber (TPC) upgrades [8].

2. Data analysis strategy

The datasets used for the analyses of different colliding systems included almost 300 million pp collisions recorded in 2010, 100 million minimum bias p–Pb collisions recorded in 2013, 17 million central events (0–10%) and 13 million semi-central (20–50%) events for Pb–Pb collisions recorded in 2011. The ALICE experimental apparatus is described in detail in [9]. The main detectors used for the dielectron analyses in the three colliding systems are the ITS (for vertexing, tracking and particle identification) [10], the TPC (for tracking and particle identification) [11] and the TOF detector (for particle identification) [12]. Events among those having the z–coordinate of

the vertex within 10 cm from the geometric center of the ALICE experiment have been selected. In Pb–Pb collisions the centrality selection has been done using the measured multiplicity in the V0 detector [13]. Most of the electrons produced in the collision originated from photon conversions in the detector material and they represented the main background source. The conversion rejection was based on single track and pair cuts. Tracks have been selected by applying strict quality requirements which included a hit in the first layer of the Silicon Pixel Detector (the innermost layer of the ITS) and tight cuts on the distance of closest approach (DCA) to the primary vertex to select primary tracks and thus reduce the contamination from secondaries. The conversion pair rejection exploited the correlation between the plane containing the electron-positron pair and the orientation of the ALICE magnetic field. Cuts have also been applied on the particle pseudorapidity ($\eta < 0.8$) to avoid edge effects, and on the transverse momentum (the minimum is set to 200 MeV/c for the analysis of pp and p–Pb collisions and to 400 MeV/c for Pb–Pb collisions). The electron identification was based on the measurement of the average energy loss per unit path length in the TPC and ITS and on the time of flight measurement in the TOF detector. The particle identification cuts have been tuned to give a high level of electron purity in order to reduce the effects of hadronic contamination on the dielectron mass spectrum (electron-hadron or hadron-hadron correlations). The background has been estimated using the like-sign spectrum multiplied by the R factor. This correction factor has been calculated as the ratio between the unlike-sign and like-sign distributions from mixed events and has been used to correct for the different acceptance of unlike-sign and like-sign pairs. The like-sign background conveniently includes both combinatorial and correlated background. The unlike-sign spectrum, after background subtraction, has been corrected for the pair efficiency that has been calculated using the Monte Carlo simulation including a realistic description of the detector effects.

3. Results in pp collisions at $\sqrt{s} = 7$ TeV

The dielectron invariant mass spectrum measured in pp collisions at $\sqrt{s} = 7$ TeV is compared to the expected overall contribution from hadronic dielectron sources (hadronic cocktail). Figure 1 left shows this comparison and the ratio of data and cocktail. The cocktail has been produced using as input the p_{T} differential cross sections of π^0, η ,ϕ and J /ψ measured by ALICE [14], while the contributions from the remaining mesons are obtained by m_{T} scaling. The $c\bar{c}$ mass distribution is obtained from PYTHIA 6, scaled to the charm cross section measured by ALICE [15]. The dielectron invariant mass spectrum is in agreement with the hadronic cocktail within the statistical and systematic uncertainties (Fig. 1 left).

In order to extract the direct virtual photon yield, the invariant mass spectrum for $p_{\mathrm{T}}^{\mathrm{ee}} \gg m_{\mathrm{ee}}$ is fit with a two component function: $f(m) = f_{dir}(m) + f_c(m)$, where f_{dir} is the invariant mass distribution of virtual direct photons and f_c is the cocktail shape in the fitting range. The fraction of virtual direct photons extracted from the fit is consistent with the measurement of real direct photons using the photon conversion method (PCM) (Fig. 2) [16]. The virtual direct photon invariant cross section is consistent with NLO pQCD calculations (Fig. 3) [17,18].

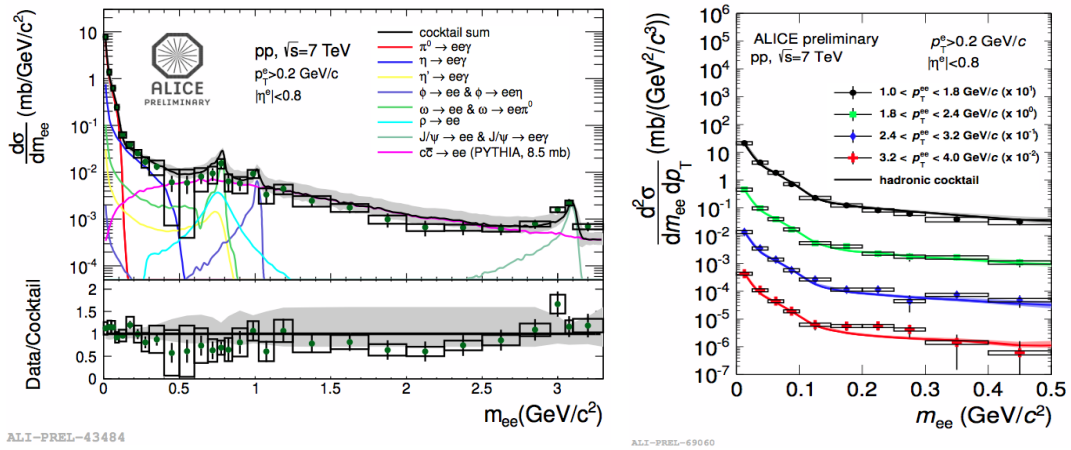

Figure 1: (Left) Dielectron invariant mass spectrum measured in pp collisions at $\sqrt{s} = 7$ TeV compared to the hadronic cocktail. (Right) Dielectron mass spectra in different p_T ranges.

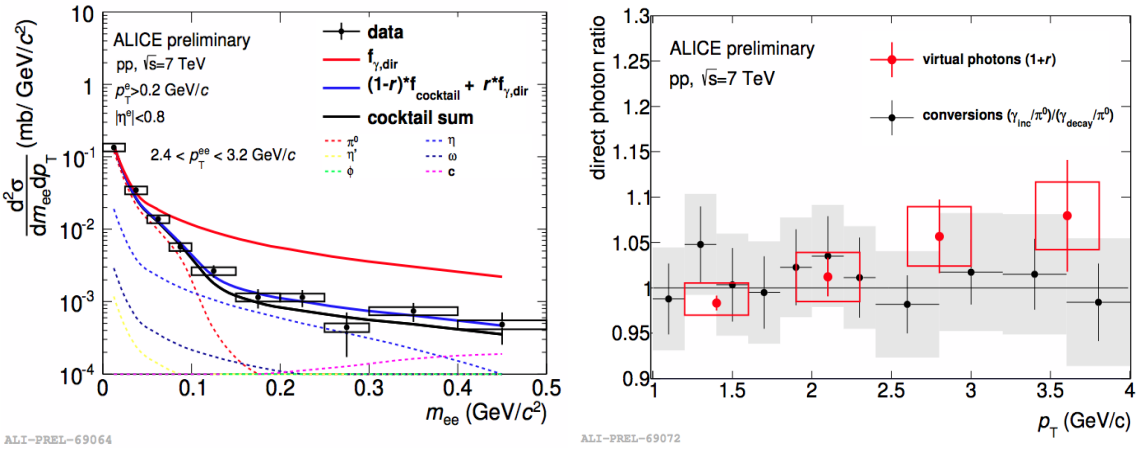

Figure 2: (Left) Two component fit to the dielectron spectrum in the low-mass region. (Right) Virtual direct photon ratio (red) compared to the results from the real photon measurement with PCM method (black) [16].

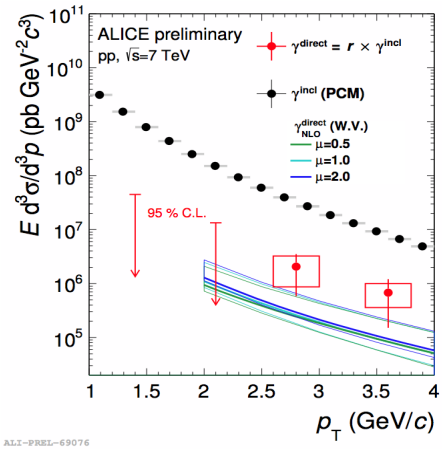

Figure 3: Inclusive photon spectrum from PCM measurement (black) and virtual direct photon invariant cross section (red) compared to NLO pQCD calculations [17,18]. Arrows indicate upper limits at 95% confidence level.

4. Results in p–Pb collisions at $\sqrt{s_{NN}} = 5.02$ TeV

Figure 4 shows the invariant mass dielectron spectrum measured in p–Pb collisions at $\sqrt{s} = 5.02$ TeV compared to the hadronic cocktail. Charged pion spectra [19] are used as cocktail input while the contributions from the other light mesons are obtained by m_T scaling. Contributions from semileptonic heavy-flavor decays and the J/ψ mesons are calculated using PYTHIA 6, tuned to the ALICE measurements in pp and p–Pb collisions. The measured dielectron invariant mass spectrum is in reasonable agreement with the cocktail over the whole mass range and in all p_T^{ee} bins within the statistical and systematic uncertainties. Data might favor a lower charm production cross section in the intermediate mass region.

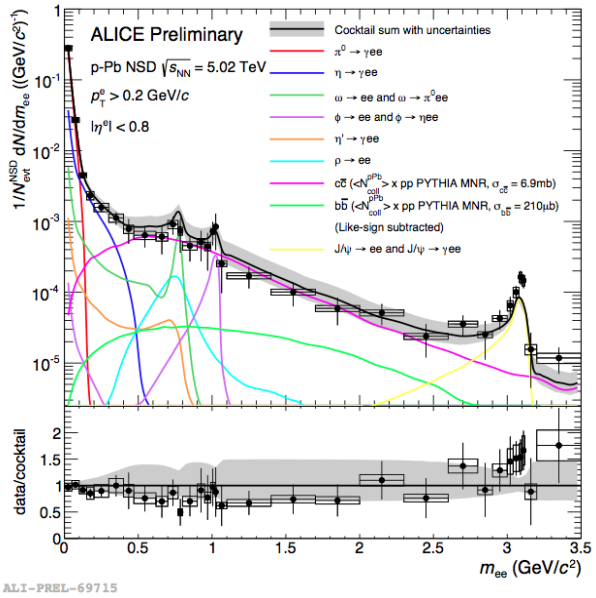

Figure 4: Dielectron invariant mass spectrum measured in p–Pb collisions at $\sqrt{s} = 5.02$ TeV compared to the hadronic cocktail.

5. Dielectron continuum in Pb–Pb collisions at $\sqrt{s_{NN}} = 2.76$ TeV

The raw dielectron invariant mass spectra in central (0–10%) and semi-central (20–50%) Pb–Pb collisions at $\sqrt{s_{NN}} = 2.76$ TeV in the transverse momentum range $1 < p_T^{ee} < 2$ GeV/c are shown in figure 5. The S/B ratio in the low-mass region ($m_{ee} < 500$ MeV/c^2) is $\sim 10^{-2}$ in semi-central and $\sim 10^{-3}$ in central collisions. This makes the dielectron measurement in Pb–Pb collisions a complicated and challenging task.

The elliptic flow v_2 of thermal photons should provide information on the QGP formation time [20], a very important parameter used for the hydrodynamical description of the system. Figure 6 shows the dielectron v_2 not corrected for efficiency in semi-central Pb–Pb collisions for different p_T^{ee} ranges.

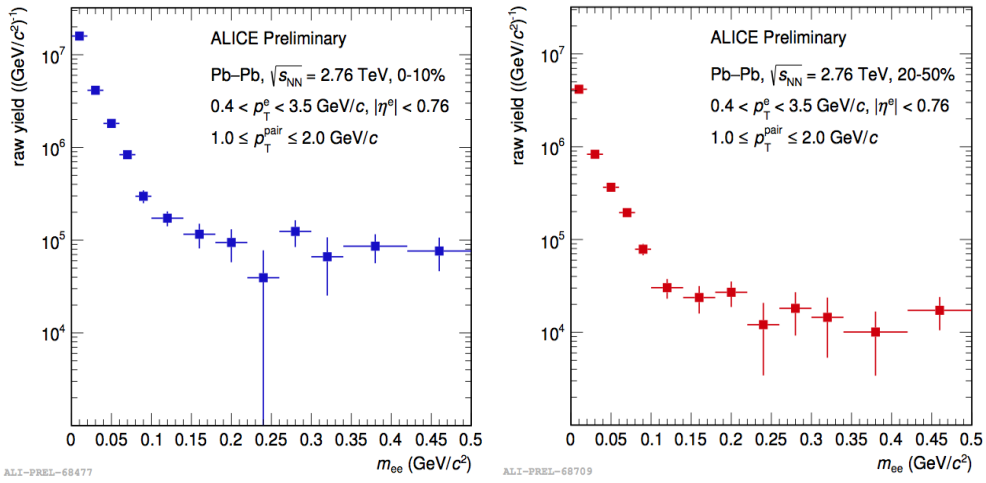

Figure 5: Raw dielectron mass spectrum measured for central (Left) and semi-central (Right) Pb–Pb collisions at $\sqrt{s_{NN}} = 2.76$ TeV.

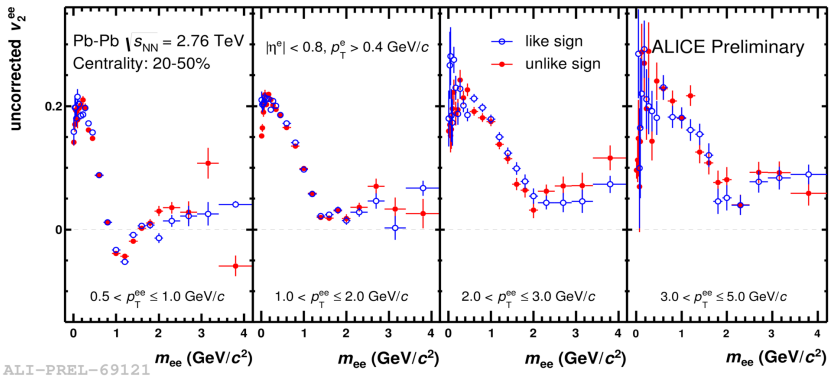

Figure 6: Uncorrected dielectron v_2 for different p_T^{ee} ranges measured in semi-central Pb–Pb collisions at $\sqrt{s_{NN}} = 2.76$ TeV.

6. Perspectives for dielectron measurements after ALICE upgrade

The ALICE upgrade program includes the installation of a new ITS and a new TPC readout system during the long shutdown 2 at the LHC. The future ITS will have seven layers of MAPS silicon detectors with reduced material budget. The first layer will be placed closer to the main interaction vertex ($\sim$ 2.2 cm) thus improving the vertexing and tracking capabilities. Moreover the new detector layout will provide a better separation of secondary tracks and improved DCA resolution. The new detector will be complemented by a faster readout system (1000 kHz for pp collisions, 100 kHz for Pb–Pb collisions). The TPC readout will be based on GEM foils that will allow a much higher data acquisition rate (up to a factor $\sim$ 100x). The performances of the upgraded ALICE experiment in the measurement of a possible thermal enhancement in the low invariant mass region have been studied for central and semi-central collisions. Figure 7 shows the expected dielectron spectra after the subtraction of the hadronic contributions, for 25 million before and 2.5 billion events after the upgrade respectively. While the measurement is dominated by uncertainties in the first case, the upgrade is expected to allow for a temperature measurement in the intermediate mass region within 10% statistical and 20% systematic uncertainty [21].

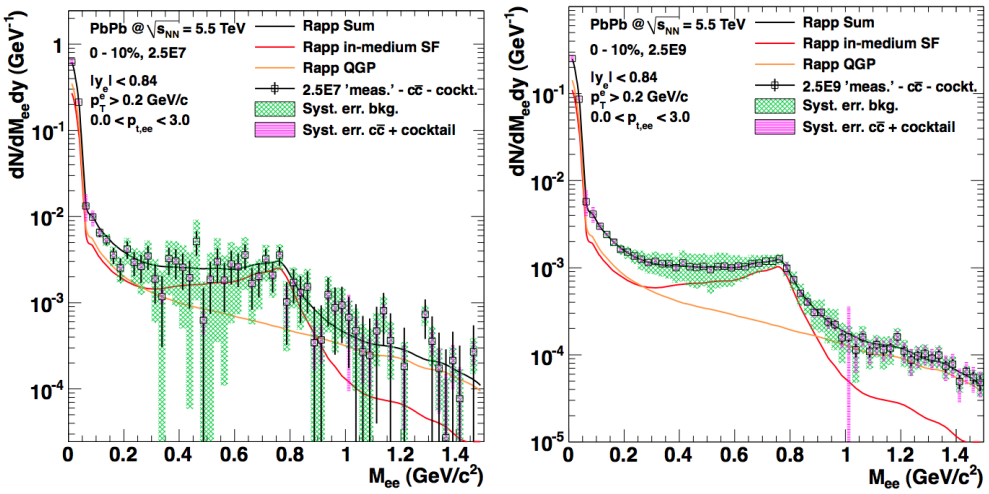

Figure 7: Expected dielectron invariant mass spectrum in Pb–Pb collisions after subtraction of hadronic sources for 25 million central events and the current detector setup (Left) and for 2.5 billion central events and the upgraded detectors (Right) [21].

7. Conclusion

Dielectron invariant mass spectra have been measured with the three different colliding systems and different energies. In pp collisions the extracted fraction of virtual direct photons is consistent with PCM measurement and the direct photon invariant cross section is consistent with NLO pQCD calculations. In p–Pb collisions the dielectron spectrum is in agreement with the hadronic cocktail within statistical and systematic uncertainties. Subtracted raw yields have been extracted for Pb–Pb collisions for two centrality classes. Further analysis is ongoing. The expected performances of the ALICE experiment after the upgrade of the main detectors have been studied. The simulations indicate an expected improved significance of the temperature measurement with upgraded detectors and an enhanced statistics in Run 3.

References

[1] J-e. Alam, S. Raha, and B. Sinha, Physics Reports, vol. 273, pp. 243–362 (1996).

[2] K. Adcox et al., Nucl. Phys. A 757, 184 (2005).

[3] T. Peitzmann, M. H. Thoma, Physics Reports, vol. 364, pp. 175–246 (2002).

[4] Physical Review C, vol. 82, no. 3, Article ID 034901 (2010).

[5] R. Rapp and J. Wambach,Advances in Nuclear Physics, vol. 25, pp. 1–205 (2000).

[6] K. Adare et al. (PHENIX Collaboration), Phys.Rev.C81:034911 (2010).

[7] CERN-LHCC-2013-024, ALICE-TDR-017

[8] CERN-LHCC-2013-020, ALICE-TDR-016

[9] JINST. 3 S08002 (2008).

[10] CERN-LHCC 99-12, ALICE-TDR-4

[11] CERN-LHCC 2000-001, ALICE-TDR-7

[12] CERN-LHCC 2000-012, ALICE-TDR-8

[13] CERN-LHCC-2004-025, ALICE-TDR-011

[14] I.Erdemir, Master Thesis, Goethe-Universitat Frankfurt am Main, Germany (2014).

[15] B. Abelev at al. (ALICE collaboration), JHEP01 128 (2012).

[16] Nucl.Phys. A904-905 573c-576c (2013).

[17] A. Adare et al., Phys.Rev.C 87, 054907 (2013).

[18] A. Adare et al., Phys.Rev.Lett. 104, 132301 (2010).

[19] Phys.Lett. B736 196-207 (2014).

[20] H.van Hees, C. Gale, R. Rapp, Phys. Rev. C 84, 054906 (2011).

[21] B. Abelev et al. (ALICE Collaboration), J. Phys. G 41 087002 (2014).